

Bulk and Spectral Observables in Lattice QCD

T Hatsuda

Department of Physics, The University of Tokyo, Tokyo 113-0033, Japan

E-mail: hatsuda@phys.s.u-tokyo.ac.jp

Abstract. We review recent developments in lattice simulations of the equation of state, order of the thermal phase transition and the determination of the pseudo-critical temperature in (2+1)-flavor QCD. Owing to the increasing computer power, new algorithms, and improved fermion formulations, studies of bulk QCD matter are approaching to the stage of precision science. We also review recent lattice studies on the spectral properties of heavy quarkoniums inside the quark-gluon plasma (QGP). Although they are still in an exploratory stage, interesting physics in relation to the strongly correlated QGP is being extracted.

1. Introduction

One of the main goals of the lattice QCD studies is to make first principle analysis of hot/dense QCD and to supply reliable inputs to quark-gluon plasma (QGP) phenomenologies [1]. Shown in Fig.1 is a schematic QCD phase diagram indicating three basic phases; the chiral symmetry broken (χ SB) phase, the color superconducting (CSC) phase and the QGP phase. Precise locations of the phase boundaries and the

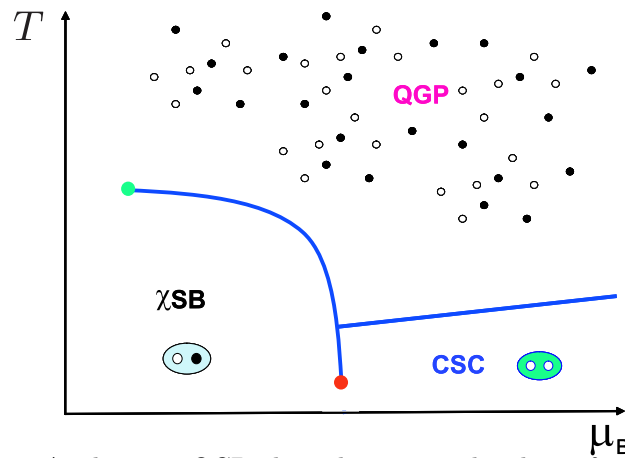


Figure 1. A schematic QCD phase diagram in the plane of temperature T and baryon chemical potential μ_B . Solid lines indicate the first order phase boundaries. Several critical points at which the first order lines terminate may exist, e.g. the high T critical point [2] and high μ_B critical point [3].

critical points as well as the dynamics in each phase should be determined by non-perturbative method such as the lattice QCD.

QCD partition function in a finite box with a spatial volume V and the lattice spacing a can be written as

$$Z(T, \mu; a, V) = \text{Tr} \left[e^{-(\hat{H} - \mu \hat{N})/T} \right] = \int [dU] F(U) e^{-S_g(U)}, \quad (1)$$

where U is the gauge field defined as an element of $SU(3)_c$ and $F(U)$ denotes the quark contribution to Z . Eventually, we need to take the continuum limit ($a \rightarrow 0$) and the thermodynamic limit ($V \rightarrow \infty$) to extract physical observables in the real world.

In the past few years, there have been considerable progress in lattice QCD approach: (i) available computer speed becomes as fast as 50 Tflops, (ii) improved fermion formulations have been tested extensively (such as stout, asqtad and p4 improved actions for staggered quarks and the clover action for Wilson quark), (iii) new fermion formulations with good chiral properties are started to be used (such as domain wall and overlap fermions), and (iv) new algorithms for full QCD simulations are proposed and implemented (such as the rational hybrid Monte Carlo method (RHMC) and the domain-decomposition hybrid Monte Carlo method (DDHMC) [5]). Shown in Fig.2 is so called the Berlin wall plot where the computational cost in unit of Tflops-year is plotted against m_π/m_ρ . The quark mass dependence of the cost becomes weaker than before, and simulations with realistic quark masses may be done in a reasonable amount of time by using O(50) Tflops machines.

In the following, we will focus on the bulk and spectral properties associated with the QCD phase transition at finite T with $\mu_B = 0$. For the developments in lattice QCD at finite chemical potential, see the recent review [4].

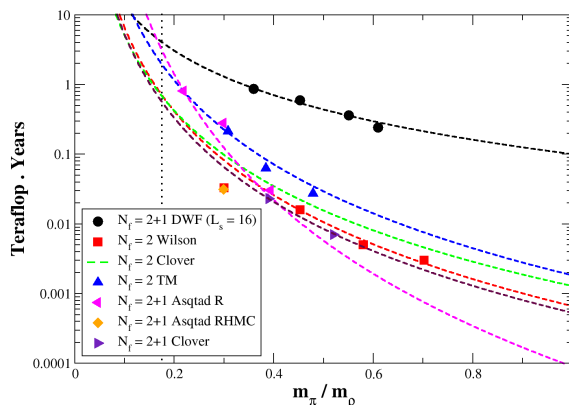


Figure 2. Updated Berlin wall plot which shows the cost to generate 1000 independent gauge configurations on $24^3 \times 40$ lattice with $a = 0.08$ fm in various fermion formulations with modern algorithms [6].

2. Equation of state in (2+1)-flavor QCD

The equation of state at finite T characterizes the bulk QCD matter. Also it becomes an fundamental input together with the transport coefficients [7] to the relativistic hydrodynamics for QCD fluid [8]. Shown in Fig.3 is the state-of-the-art calculation of the energy density ε as a function of T in (2+1)-flavor QCD with asqtad improved staggered quarks. (See also the recent results for 3-flavor QCD with the p4 action [10] and for (2 + 1)-flavor QCD with the stout action [11].)

The figure shows that ε/T^4 increases rapidly at $T \sim 200$ MeV and approaches the Stefan-Boltzmann (SB) limit from below. The deviation from the SB limit at high T is due to the quark-gluon interaction which decreases only logarithmically as T increases. Quantitative understanding of the deviation is a non-trivial issue and cannot be treated in naive thermal perturbation [13].

3. Order of the transition in (2+1)-flavor QCD

Using the pressure $P(\vec{K}) = (T/V) \cdot \ln Z$ and a vector $\vec{K} \equiv (T, \mu, m_q, a, V, \dots)$, one may define the n -th order transition as the one where non-analyticity of P in the thermodynamic limit ($V \rightarrow \infty$) first appears in the n -th derivative of P with respect to \vec{K} . For example, if $(\partial/\partial T)P = s$ is discontinuous at certain T , it is the first order transition. On the other hand, if $(\partial/\partial T)P$ is continuous and $(\partial/\partial T)^2 P = (\partial/\partial T)s = c_v/T$ diverges at certain T , it is an example of the second order transition. If smooth

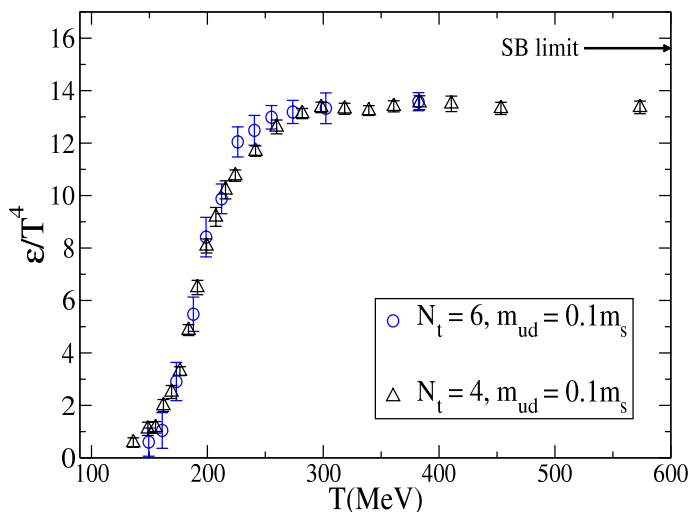


Figure 3. Energy density ε as a function of T for (2+1)-flavor QCD with asqtad improved action on the lattice, $N_t \times N_s^3 = 4 \times (12^3 - 16^3)$ and $6 \times (12^3 - 20^3)$ [9]. The strange quark mass m_s is about the physical value, while the light quark mass $m_{ud} \simeq 0.1m_s$ corresponding to $m_\pi/m_\rho \simeq 0.3$. The Sommer scale $r_1 = 0.138(7)(4)$ fm is used to set the scale. Lattice spacing at $T \simeq 200$ MeV is 0.247 (0.165) fm for $N_t = 4$ (6).

phase change takes place without the non-analyticity of P , it is the crossover. To make a distinction between the phase transition and the crossover from the numerical simulations, the scaling behavior of certain observables as a function of V needs to be studied (the finite size scaling analysis) [17]. In the (2+1)-flavor QCD, the relevant observable is the chiral susceptibility whose volume dependence at its maximum reads

$$\chi_m = (\partial/\partial m_{\text{ud}})^2 P \rightarrow V^\alpha \text{ at the peak,} \quad (2)$$

where $\alpha \simeq 1$ ($2/3$) for the first (second) order transition, and $\alpha \simeq 0$ for crossover.

Shown in the left panel of Fig.4 is the dimensionless chiral susceptibility χ_m/T^2 around its peak for different values of the dimensionless volume $N_s = V/a^3 = 18^3, 24^3, 32^3$ for (2+1)-flavor QCD with realistic masses of u, d, s quarks [12]. There is no appreciable volume dependence for the height of the susceptibility, which suggests the crossover nature. The right panel of Fig.4 shows the subtracted chiral susceptibility in the continuum limit $\Delta\chi$ (= the peak of $\chi_m(T) - \chi_m(0)$) in a renormalization group invariant combination $T^4/(m_{\text{ud}}^2\Delta\chi)$ as a function of the dimensionless inverse-volume, $1/(T_c^3V)$. The height of the susceptibility approaches to a non-vanishing constant in the thermodynamic limit and has different scaling behavior from those of first or second order transitions. This gives a strong evidence that the hadron-QGP transition at finite T with zero chemical potential is a crossover in the real world.

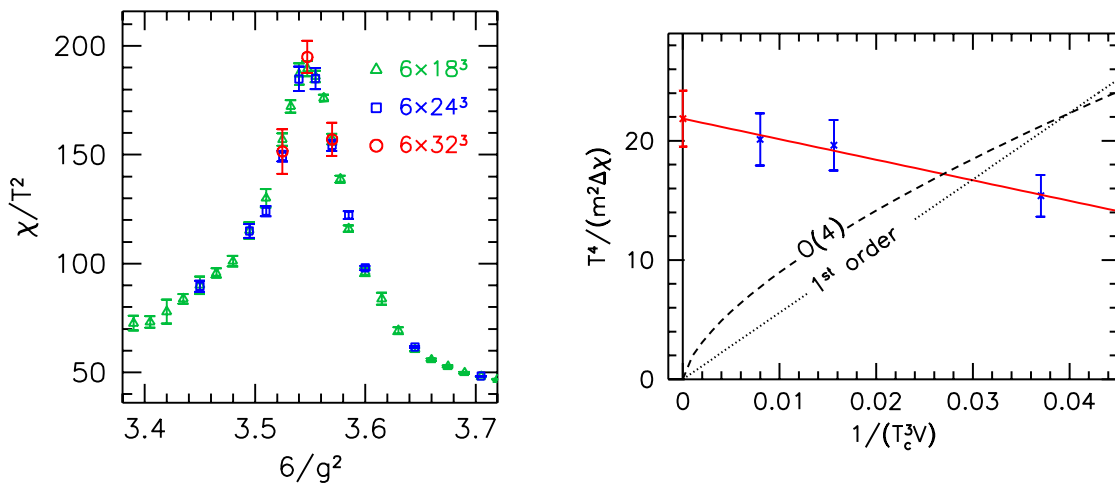


Figure 4. Left: The chiral susceptibility in (2+1)-flavor QCD as a function of the bare coupling, $6/g^2$, for different values of the spatial volume, $N_t^3 = V/a^3 = 18^3, 24^3, 32^3$. The stout improved staggered fermion action is employed and the quark masses are chosen to reproduce $m_K/m_\pi=3.689$ and $f_K/m_\pi=1.185$. Right: The volume dependence of the peak of the subtracted chiral susceptibility in the continuum limit. Dotted (dashed) line is an expectation from the first order (second order) phase transition. Figures are taken from [12].

4. Pseudo-critical temperature for (2+1)-flavor QCD

Since the hadron-QGP transition in the real world is crossover, the “critical” temperature T_c is not a well-defined concept. Nevertheless, one may introduce a “pseudo-critical” temperature T_{pc} as a peak position of certain susceptibility. The actual value of T_{pc} is different for different choice of susceptibility, e.g. $\chi_m = (\partial/\partial m_{ud})^2 P$, $\chi_T = (\partial/\partial T)^2 P$, and $\chi_{mT} = (\partial^2/\partial m \partial T) P$. Note also that multiplying an arbitrary function of m_{ud} and T to the susceptibilities can change the value of T_{pc} .

Shown in Fig.5 is a summary of (pseudo-)critical temperature recently calculated from the dimensionless chiral susceptibility, χ_m/T^2 , for (2+1)-flavor QCD. Extrapolation to the continuum limit is taken by using the data for several values of N_t . The upper two bars are T_c with different extrapolations to the chiral limit $m_{ud} = 0$ by MILC collaboration [14]. The middle bar is T_{pc} extrapolated to the realistic m_{ud} by RBC-Bielefeld collaboration [15]. The lower bar is T_{pc} calculated at the realistic m_{ud} by Wuppertal-Budapest collaboration [16]. Note that different improved actions and different scale determinations are adopted in three groups. When extracting T_{pc} in MeV unit, we need to use the chain rule:

$$T_{pc} = \left(\frac{T_{pc}(a)}{a^{-1}} \right)_{a \rightarrow 0} \cdot \left(\frac{a^{-1}}{M(a)} \right)_{a \rightarrow 0} \cdot M^{\text{“exp”}}. \quad (3)$$

Here M , which has a dimension of mass, is chosen either to be a direct physical observable (such as m_ρ , f_π and f_K) or to be a semi-empirical quantity (such as the Sommer scales $1/r_0$ and $1/r_1$ defined from the heavy-quark potential through $r^2 dV(r)/dr|_{r=r_0} = 1.65$ and $r^2 dV(r)/dr|_{r=r_1} = 1.0$).

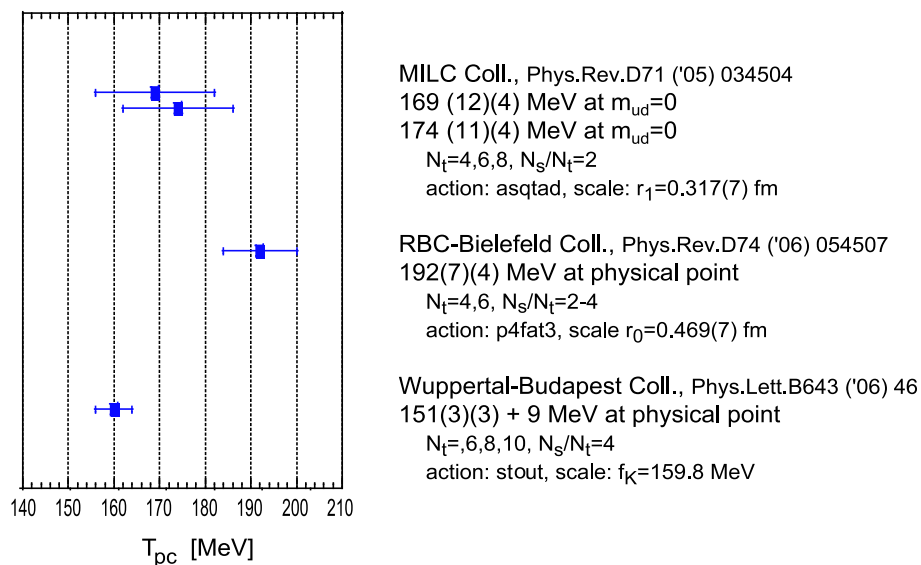


Figure 5. Recent determinations of the (pseudo-)critical temperature for (2+1)-flavor QCD with staggered quarks. As for the lowest bar, we add 9 MeV to make a comparison to other results obtained from χ_m/T^2 [16].

There are a number of issues to be studied further before drawing definite conclusion on the value of T_{pc} in the real world. In particular, (i) careful continuum extrapolation ($a \rightarrow 0$) by the data with larger N_t , (ii) determination of T_{pc} in the case of Wilson fermion [18], and (iii) resolving the difference between the Sommer scale in the continuum limit obtained from a being determined by the 2S-1S mass splitting of the bottomonium with staggered quark ($r_0 = 0.468(7)$ fm) [19] and that obtained from a being determined by the kaon mass with Wilson quark ($r_0 = 0.516(21)$ fm) [20].

5. Heavy quarks inside QGP

Heavy quarks in the real world (such as the charm and bottom) have finite masses and may receive substantial kick from the light plasma-constituents which have typical energy of about $3T$. Therefore, it is important to examine the dynamical correlations (both spatial and temporal) of the heavy quarks inside QGP. It is also relevant to study the modification of the heavy quarkonium properties in hot QCD matter [21].

5.1. Charmonium wave function in quenched QCD

An attempt to study the J/Ψ wave function at finite temperature in quenched QCD ($F(U)$ is take to be unity in Eq.(1)) on an anisotropic lattice was performed by Umeda et al. [22]. They have studied the equal-time Bethe-Salpeter wave function $w(\vec{r}, \tau)$ at finite T in the Coulomb gauge. In Fig.6, the normalized wave function, $\phi(\vec{r}, \tau) = w_i(\vec{r}, \tau)/w_i(\vec{0}, \tau)$ is plotted below and above T_c for various time slices. The black dashed line is the wave function prepared at $\tau = 0$. For free quarks without gauge

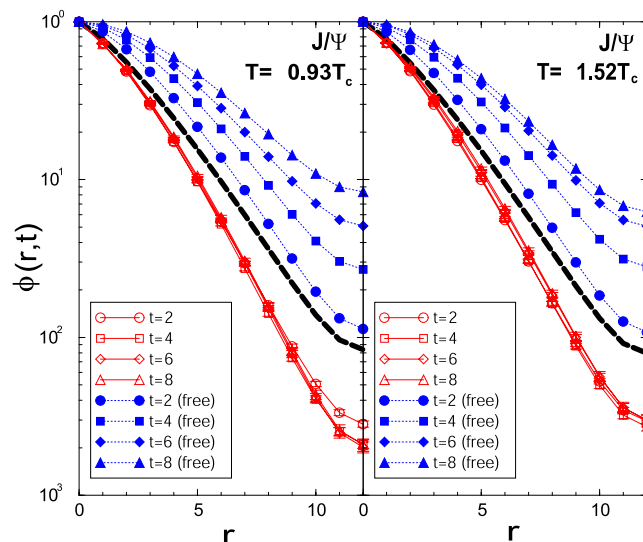


Figure 6. The equal-time Bethe-Salpeter wave function normalized at the origin as a function of the spatial separation r between the charm and the anti-charm. Blue (red) points correspond to free (interacting) quarks [22]. The black dashed line is the wave function initially prepared at $\tau = 0$. Note that $t \equiv \tau$ in this figure.

interactions, the wave function becomes broader as the imaginary time τ increases. On the other hand, the wave function for the interacting system is almost unchanged even at $T = 1.52T_c$, which suggests that J/Ψ may survive as a bound state in the deconfined phase.

5.2. Charmonium spectral function in quenched QCD

The spectral functions of hadronic correlators give us another information on hadronic modes at finite T as originally suggested in [23]. The spectral function $\sigma(\omega, \vec{p})$ for hadronic correlation may be defined through the spectral decomposition:

$$D(\tau, \vec{p}) = \int_{-\infty}^{+\infty} \frac{e^{-\tau\omega}}{1 \mp e^{-\omega/T}} \sigma(\omega, \vec{p}) d\omega \quad (0 \leq \tau < T^{-1}). \quad (4)$$

The maximum entropy method (MEM) provides an efficient and powerful way to obtain a unique σ from the lattice data D without making a priori parameterization [24].

Applications of MEM to the $s\bar{s}$ mesons at finite T [25] and to the charmoniums at finite T [26, 27, 28, 29] within the quenched QCD have been carried out and it was shown that the J/Ψ and η_c survive even above T_c as distinct peaks. Shown in the left (right) panel of Fig.7 is the dimensionless spectral function for J/Ψ (η_c) below and above T_c on $32^3 \times (96 - 32)$ ($24^3 \times (160 - 34)$) anisotropic lattices with the spatial volume $V = (1.25\text{fm})^3$ ($V = (1.34\text{fm})^3$) taken from Ref.[26] (Ref.[29]). The figures indicate that the low-lying s-wave resonances still survive even at $1.5 T_c$, which is consistent with the result in Fig.6. Note that this result is not an artifact of the small spatial volume, which was carefully checked in [30].

There are several topics which are interesting to be studied within the quenched QCD, such as the spectral functions of the charmoniums moving inside the hot medium [31] and the spectral functions of bottomoniums above T_c [32].

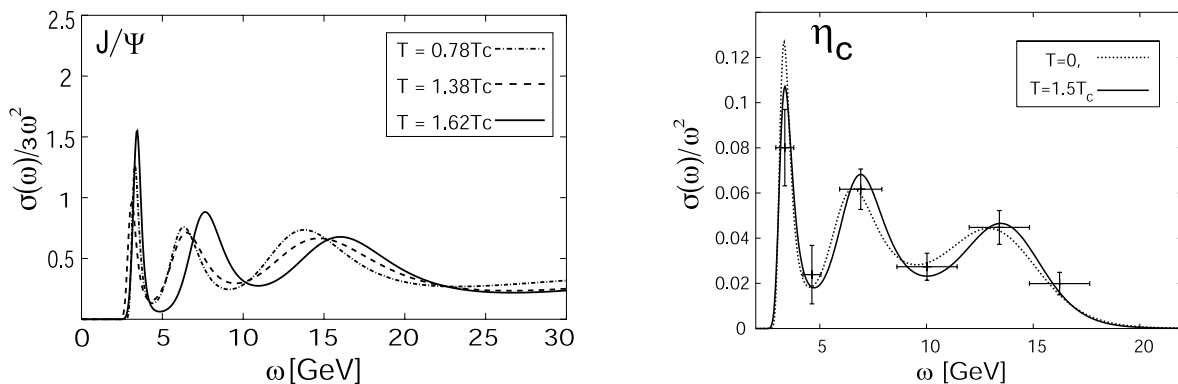


Figure 7. Left: Spectral functions measured in quenched QCD simulations on an anisotropic lattice with the spatial volume $(1.25 \text{ fm})^3$ for the J/Ψ channel [26]. Right: Spectral functions measured in quenched QCD simulations on an anisotropic lattice with the spatial volume $(1.34 \text{ fm})^3$ for the η_c channel [29].

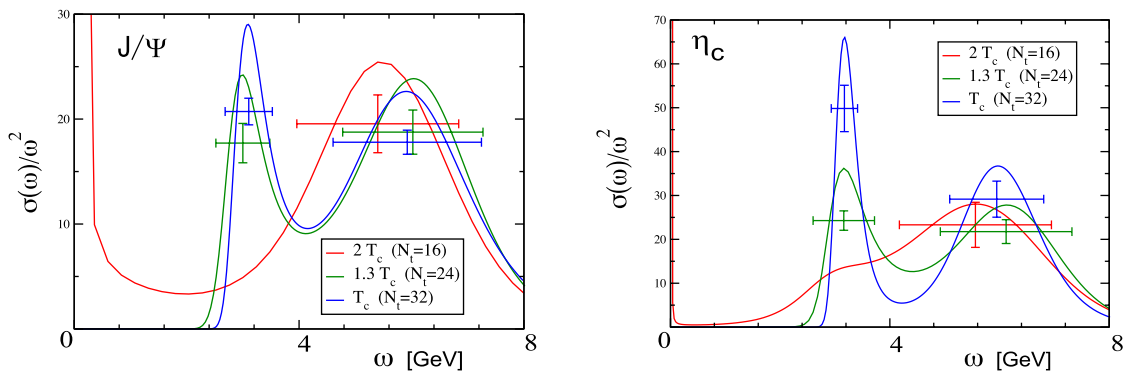


Figure 8. Spectral functions in the vector and pseudo-scalar channels in 2-flavor QCD on $8^3 \times (32 - 16)$ anisotropic lattices. The spatial lattice volume is $V \sim (1.2 \text{ fm})^3$ and the light quark mass corresponds to $m_\pi/m_\rho \sim 0.5$. The figures are adapted from [34].

5.3. Charmonium spectral function in 2-flavor QCD

In quenched QCD, only gluons are thermally excited in the plasma, while, in full QCD, both quarks and gluons are thermally active. Because the number of degrees of freedom increase in full QCD, the dissociation rate of the charmoniums will be larger. On the other hand, the pseudo-critical temperature T_{pc} in full QCD (160-200 MeV) is substantially smaller than $T_c \sim 270$ MeV in quenched QCD. Due to the compensation of these effects, the ratio of the dissociation temperature T^* and the (pseudo-)critical temperature in full QCD is not much different from the ratio in quenched QCD and could take a value of around 2 [33].

Aarts et al. has recently reported an exploratory study of 2-flavor QCD on $8^3 \times (32 - 16)$ anisotropic lattices [34]. Shown in Fig.8 are the spectral functions of the J/Ψ and η_c . The results suggest that, even with the thermal excitations of light quarks, the low-lying charmoniums may survive inside the quark-gluon plasma above T_c until they dissociate away around $2T_{pc}$.

6. Summary

We reviewed recent developments in lattice simulations on the equation of state, crossover nature of the thermal phase transition and the determination of the pseudo-critical temperature in (2+1)-flavor QCD. Recent lattice results on the spectral properties of the heavy quarkoniums inside the quark-gluon plasma are also summarized.

Acknowledgements: This work was partially supported by Japanese MEXT Grant No. 18540253. The author thanks T. Umeda, S. Ejiri, F. Karsch and Z. Fodor for useful information and discussions.

References

- [1] Yagi K, Hatsuda T and Miake Y 2005 *Quark-Gluon Plasma*, (Cambridge Univ. Press, Cambridge).
- [2] Asakawa M and Yazaki K 1989 *Nucl. Phys.* **A504** 668.
Barducci A *et al.* 1989 *Phys. Lett.* **B231** 463.
- [3] Hatsuda T, Tachibana M, Yamamoto N, and Baym G 2006 *Phys. Rev. Lett.* **97** 122001.
- [4] Schmidt C 2006 *PoS LAT2006* 021 [hep-lat/0610116].
- [5] Kennedy A D 2006 *arXiv*: hep-lat/0607038. Del Debbio L *et al.* 2006 *arXiv*: hep-lat/0610059.
- [6] Clark M A 2006 *arXiv*: hep-lat/0610048.
- [7] Sakai S and Nakamura A 2006 *PoS LAT2005* 186 [hep-lat/0510100].
- [8] Hirano T and Gyulassy M 2006 *Nucl. Phys.* **A769** 71.
- [9] Bernard C *et al.* 2006 *arXiv*: hep-lat/0611031.
- [10] Karsch F 2006 *J. Phys. Conf. Ser.* **46** 122.
- [11] Aoki Y, Fodor Z, Katz S D and Szabo K K 2006 *JHEP* **0601** 089.
- [12] Aoki Y, Endrodi G, Fodor Z, Katz S D, and Szabo K K 2006 *Nature* **443** 675.
- [13] Kraemmer U and Rebhan A 2004 *Rept. Prog. Phys.* **67** 351.
- [14] Bernard C *et al.* 2005 *Phys. Rev.* **D71** 034504.
- [15] Cheng M *et al.* 2006 *Phys. Rev.* **D74** 054507.
- [16] Aoki Y, Fodor Z, Katz S D, and Szabo K K 2006 *Phys. Lett.* **B643** 46.
- [17] Ukawa A 1993 *Lectures on Lattice QCD at Finite Temperature*, (Uehling Summer School, Seattle).
- [18] Maezawa Y *et al.* 2007 *arXiv*: hep-lat/0702005.
- [19] Gray A *et al.* (HPQCD and UKQCD Coll.) 2005 *Phys. Rev.* **D72** 094507.
- [20] Ishikawa T *et al.* (CP-PACS and JLQCD Coll.) 2006 *PoS LAT2006* 181 [hep-lat/0610050].
- [21] Matsui T and Satz H 1986 *Phys. Lett.* **B178** 416.
Hashimoto T, Hirose K, Kanki T and Miyamura O 1986 *Phys. Rev. Lett.* **57** 2123.
- [22] Umeda T, Katayama R, Miyamura O and Matsufuru H 2001 *Int. J. Mod. Phys.* **A16** 2215.
- [23] Hatsuda T and Kunihiro T 1985 *Phys. Rev. Lett.* **55** 158. DeTar C 1985 *Phys. Rev.* **D32** 276.
- [24] Asakawa M, Hatsuda T and Nakahara Y 2001 *Prog. Part. Nucl. Phys.* **46** 459.
- [25] Asakawa M, Hatsuda T and Nakahara Y 2003 *Nucl. Phys. Proc. Suppl.* **119** 481.
- [26] Asakawa M and Hatsuda T 2004 *Phys. Rev. Lett.* **92** 012001; *J. Phys.* **G30** S1337.
- [27] Datta S, Karsch F, Petreczky P and Wetzorke I 2004 *Phys. Rev.* **D69** 094507.
- [28] Umeda T, Nomura K and Matsufuru H 2005 *Eur. Phys. J.* **C39S1** 9.
- [29] Jakovac A, Petreczky P, Petrov K and Velytsky A 2007 *Phys. Rev.* **D75** 014506.
- [30] Iida H, Doi T, Ishii N, Suganuma H and Tsumura K 2006 *Phys. Rev.* **D74** 074502.
- [31] Datta S, Karsch F, Wissel S, Petreczky P and Wetzorke I 2004 *arXiv*: hep-lat/0409147.
Aarts G, Allton C, Foley J, Hands S and Kim S 2006 *arXiv*: hep-lat/0610061.
- [32] Datta S, Jakovac A, Karsch F and Petreczky P 2006 *AIP Conf.Proc.* **842** 35 [hep-lat/0603002].
- [33] Hatsuda T T 2006 *Int. J. Mod. Phys.* **A21** 688 [hep-ph/0509306].
- [34] Aarts G *et al.* 2006 *PoS LAT2006* 126 [hep-lat/0610065].